Peer-reviewed version available at Genes 2018, 9, 71; doi:10.3390/genes9020071

Article

Transcriptomic Analysis Provides Insights into Grafting Union Development in Pecan (*Carya illinoinensis*)

Zhenghai Mo [1], Gang Feng [1], Wenchuan Su [1], Zhuangzhuang Liu [1] and Fangren Peng [1,*]

[1] College of Forestry, Nanjing Forestry University, Nanjing 210037, China; m15895892025@163.com (Z.M.); 936896549@qq.com (G.F.); 997905639@qq.com (W.S.); 840574471@qq.com (Z.L.)
* Correspondence: frpeng@njfu.edu.cn; Tel.: +86-025-85427995

Abstract: Pecan (*Carya illinoinensis*), as a popular nut tree, is widely planted in China in recent years. Grafting is an important technique for its cultivation. For a successful grafting, graft union development generally involves the formation of callus and vascular bundles at the graft union. To explore the molecular mechanism of graft union development, we applied high through-put RNA sequencing to investigate transcriptomic profiles of graft union at four time points (0d, 8d, 15d, and 30d) during pecan grafting process. We identified a total of 12,180 differentially expressed genes. In addition, we found that the content of auxin, cytokinin and gibberellin were accumulated at the graft unions during the grafting process. Correspondingly, genes involved in those hormone signaling were found to be differentially expressed. Interestingly, we found that most genes associated with cell division were up-regulated at callus formative stages, while genes related to cell elongation, secondary cell wall deposition, and programmed cell death were generally up-regulated at vascular bundle formative stages. In the meantime, genes responsible for reactive oxygen species were highly up-regulated across the graft union developmental process. These results will aid in our understanding of successful grafting in the future.

Keywords: Grafting; Pecan; Transcriptome; Graft union; Hormone

1. Introduction

Pecan (*Carya illinoinensis*), a member of Juglandaceae family, is an economically important nut tree native to North America. It has been introduced to China for more than 100 years, however, for a long time, there was little incentive for its commercial planting due to an extremely long juvenile stage, with 10-15 years to maturity. Grafting is an effective approach to shorten the duration of vegetative growth, by which, pecan can start to bear fruits within 5-8 years. For the trees in Juglandaceae family, grafting is more difficult in comparison to other fruit trees. In recent years, patch budding, one of the commonly used grafting methods, conducted from July to September in China achieves over 90% grafting success [1], which makes large-scale cultivation of pecan possible. An in-depth understanding of the mechanism underlying successful grafting will help in increasing the production efficiency of pecan as well as other trees in the future.

When grafting is performed, the grafted partners, scion and rootstock, are cut and joined together. Once the scion and rootstock come into intimate contact, an intricate structural and biochemical response would happen at the graft union for a successful graft. For woody trees, following the initial adhesion of grafted partners, the graft union undergoes two essential developmental processes: the formation of callus tissues and the sufficient connection of functional vascular bundles between the scion and rootstock [2,3]. Therefore, graft union development is a process that involves cell division and differentiation at the graft junction.

Currently, reports regarding the molecular mechanism of graft union development are still limited. A cDNA-AFLP method was applied to investigate the gene expression in the graft process of hickory, and the research obtained 49 differentially expressed genes that were related to signal transduction, auxin transportation, metabolism, cell cycle, wound response and cell wall synthesis

[4]. In the hypocotyl grafts of *Arabidopsis*, changes in global gene expression were evaluated 24 h after grafting, and graft union development was revealed to involve signal transduction as well as cellular debris elimination [5]. In grapevine autografts, transcriptional changes were examined via whole genome microarray analysis, and the results revealed that graft union development triggered numerous gene expression changes related to wounding, cell wall modification, hormone signaling and secondary metabolism [6]. Comparison the gene expression between the hetero- and autografts of grapevine indicated that genes involved in stress responses were up-regulated [7]. In recent years, RNA sequencing (RNA-seq) is a rapidly emerging transcriptome technology that can perform without a reference genome. It has been employed to analysis the expression of mRNA and miRNA in hickory graft process, through which, candidate genes involved in the auxin and cytokinin signaling were identified [8], otherwise, a total of 12 candidate grafting-responsive miRNA were detected [9]. A comparative proteomic analysis of the hickory graft unions revealed that key enzymes involved in flavonoid biosynthesis were up-regulated 7 d after grafting [10].

Previously, we have paid our attention on the morphological and proteomic changes in pecan homografts [11]. However, to the best of our knowledge, there were still no reports describing genes and gene networks underlying graft union development of pecan. In this study, we applied RNA-seq technology to construct mRNA libraries from the graft unions that were collected at 0, 8, 15, and 30 days after grafting, and analyzed the transcriptomic changes across the graft process.

2. Materials and Methods

2.1. Plant material and grafting procedures

Pecan homografts were made in August using patch budding at the experimental orchard of Nanjing Forestry University (China). Graft unions (approximately 3-cm in length, the budding segment that includes the tissues of scion and the developing xylem of rootstock) were collected at 0, 8, 15, and 30 days after grafting and immediately frozen in liquid nitrogen. The sampling time points were determined according to our histological analysis of the graft union developmental process in pecan homografts. In detail, the samples at 8d, 15d and 30d were selected for exploring the differentially expressed genes that involved in the initial callus proliferation, massive callus proliferation accompanied by cambium establishment, and functional vascular bundles formation, respectively. Samples at 0d were those graft unions that collected immediately from scion and rootstock before grafting and were used as controls. Three biological replicates were performed for each time point.

2.2. RNA extraction, library construction and sequencing

Total RNA was isolated from the graft unions using the Universal Plant RNA Kit (BioTeke, Beijing, China) and treated with RNase-free DNase I (Takara) to degrade genomic DNA. RNA quality and quantity were monitored by Nanodrop 1000 Spectrophotometer (Thermo Fisher Scientific, Wilmington, DE) and Agilent 2100 Bioanalyzer (Agilent Technologies, Santa Clara, CA). For each sample, about 3 μg of the total RNA that passed the quality examinations was used for preparation of the cDNA library. Construction of sequencing libraries was performed by NEBNext® UltraTM RNA Library Prep Kit for Illumina® (NEB, Ipswich, MA, USA) according to the protocol. Briefly, the mRNA was enriched by oligo (dT)-attached magnetic beads and fragmented into short pieces, which were taken as templates for the first-strand and second-strand cDNA synthesis. And then the exonuclease/polymerase was used to convert the remaining overhangs into blunt ends. The resulting fragments were end-repaired by inserting an 'A' base to the 3' ends of the cDNA. NEBNext adopters with hairpin loop structure were then ligated to the fragments. The library fragments were purified by AMPure XP system (Beckman Coulter, Beverly, USA) to select suitable cDNA fragments. Then, the products were amplified by PCR to create sequencing libraries. The constructed libraries were sequenced by Illumina HiSeqTM 4000 platform (Biomarker Technology Company, Beijing, China).

Peer-reviewed version available at Genes 2018, 9, 71; doi:10.3390/genes9020071

The sequencing raw data has been deposited in NCBI Sequence Read Archive (SRA) with the accession number SRP118757.

2.3. De Novo Assembly and functional annotation

After RNA sequencing, adapter sequences, ploy-N reads and low quality reads from raw data were removed by in-house perl scripts to obtain clean reads. The resulting clean reads from all the samples were pooled for generating reference genes as far as possible. Trinity software with a k-mer length of 25 and other default parameters was used in the subsequent de novo assembly of transcriptome. Clean reads were assembled into contigs, and then were further linked into transcripts through pair-end joining. The produced transcripts were clustered with TGI clustering tool and the longest transcripts were recognized as unigenes. For functional annotation, unigenes were compared against the following databases, including NCBI non-redundant protein (Nr), Clusters of Orthologous Groups of proteins (COG), euKaryotic Orthologous Groups (KOG), Gene ontology (GO), Kyoto Encyclopedia of Genes and Genomes (KEGG), Protein family (Pfam) and Swiss-Prot using the BLASTX program with E-value of 10^{-5}.

2.4. Analysis of differentially expressed genes (DEGs)

The clean reads sequenced from each sample were mapped back to the unigene library. To quantify the gene expression level, FPKM (fragments per kilobase of exon per million mapped reads) was calculated in each sample by RSEM. Differential expression analysis was then performed using the DESeq R package for three comparisons (8d vs 0d, 15d vs 0d, and 30d vs 0 d). The false discovery rate (FDR) was applied to identify the P value threshold in multiple test and analysis. Only genes with FDR < 0.01 and more than two-fold change in expression between samples were considered as DEGs. GO enrichment analysis of DEGs was carried out by the topGO R package based on hypergeometric test. Additionally, we used KOBAS software to test the enriched pathway of DEGs. GO terms and KEGG pathways with corrected P value ≤ 0.01 were recognized as significantly over-represented.

2.5. Validation of RNA-seq data by quantitative real-time PCR (qRT-PCR)

RNA preparation with three biological replicates for each sample was conducted as described above. First-strand cDNA synthesis was performed using Prime-Script™ II First Strand cDNA synthesis kit (Takara Bio, Dalian, China) according to the manufacturer's instructions. The primer sets for each unigene were designed by Primer Premier 5.0, and their sequences were listed in Table S1. qRT-PCR was carried out on an ABI 7500 Real-Time PCR System (Thermo Fisher Scientific, Inc. Waltham, MA, USA) with SYBR Premix Ex Taq™ II kit (Takara). Expression was calculated as $2^{-\Delta\Delta Ct}$ and normalized to that of the reference gene Actin.

2.6. Detection of hormones content by ELISA

Samples were taken from the graft union 0, 8, 15, and 30 days after grafting with three biological replicates. The contents of endogenous indole-3-acetic acid (IAA), zeatin riboside (ZR), and Gibberellin (GA) were measured with enzyme linked immunosorbent assay (ELISA). The hormone ELISA kits were developed from China Agricultural University, which have been validated with GC-MS and HPLC method. The determination of hormone content was performed as outlined by [12].

3. Results and Discussion

3.1. De novo assembly and functional annotation

To gain a comprehensive overview of transcriptome associated with graft union development in pecan, samples at different time points (0d, 8d, 15d, and 30d after grafting) with three biological

replicates were subjected to illuminate sequencing. Raw reads were clean to generate a total of 312.08 million high-quality reads, encompassing 93.22 gigabase pairs with an average GC percentage of 46.41%. As a whole, all libraries showed good sequencing quality with Q30 more than 86.58% (Table S2). After sequence cleaning, reads from all samples were mixed to perform de novo assembly by Trinity software. Short reads were assembled into 140,455 transcripts with N50 length of 1,905 bp and an average length of 1178 bp. There were 31,127 (22.16%) transcripts in the range between 1000 bp to 2000 bp, and 25,188 (17.93%) with length more than 2000bp. All transcripts were subsequently clustered to yield 83,693 unigenes with N50 length of 1,350 bp and mean length of 892 bp. Among these, 13,698 (16.37%) unigenes were in the range of 1000-2000 bp, and 8,364 (9.99%) exceeded 2000 bp (Table 1).

Table 1. Summary for the graft union transcriptome.

	Transcript	Unigene
Total number	140,455	83,693
Total length	165,440,800 bp	74,679,367 np
N50 length	1,905 bp	1,350 bp
Mean length	1,178 bp	892 bp
200-300 bp	18,665(13.29%)	15,637(18.68%)
300-500 bp	28,705(20.44%)	21,661(25.88%)
500-1000 bp	36,770(26.18%)	24,333(29.07%)
1000-2000 bp	31,127(22.16%)	13,698(16.37%)
2000+ bp	25,188(17.93%)	8,364(9.99%)

All the 83,693 unigenes were aligned with available protein databases using BLASTx algorithm with E-value of 10-5. The results showed that there were 11,762 (14.05%) unigenes matched in the COG database, 23,260 (27.79%) in the GO database, 13,859 (16.56%) in the KEGG database, 21,612 (25.82%) in the KOG database, 25,909 (30.96%) in the Pfam database, 23,243 (27.77%) in the Swiss-Prot database, and 38,793 (46.35%) in the NR database. In total, there were 40,069 unigenes annotated in at least one database, accounting for 47.88% of all unigenes (Table 2). There were a relatively large portion of unigenes had no significant hits to current known proteins, which might represent novel genes in pecan. For functional classification of the assembled unignenes, COG and GO annotation were carried out to gain the distributions of functional categories (Fig S1).

Table 2. Summary for the annotation of unigenes.

Annotated databases	Unigene number	Percentage (%)	300 nt ≤ Length < 1000 nt	Length ≥1000 nt
COG	11,762	14.05	3,747	6,644
GO	23,260	27.79	9,028	10,879
KEGG	13,859	16.56	5,567	6,557
KOG	21,612	25.82	8,184	10,759
Pfam	25,909	30.96	8,838	14,658
Swiss-Prot	23,243	27.77	8,711	12,071
NR	38,793	46.35	15,816	17,494
Annotated in at least one database	40,069	47.88	16,463	17,751

3.2. Analysis of DEGs in the graft process of pecan

Clean reads from the 12 libraries were aligned to the obtained unigenes and quantified to calculate the expression levels by fragments per kilobase of transcript per million fragments mapped reads (FPKM). Based on the FPKM values of all genes, the correlations between each of the two samples was analyzed. And we found that there were strong correlations among biological repetitions, with the correlation coefficients over 0.90 (Fig S2).

According to the criteria of at least two-fold change and FDR < 0.01, a total of 3,470 DEGs were discovered by analyzing 8d/0d, with 2,154 up-regulated and 1,316 down-regulated; 4942 DEGs were identified in the comparison of 15d/0d, with 2,750 up-regulated and 2,192 down-regulated; 9,145 DEGs were found by comparing 30d/0d, with 3,001 up-regulated and 6,144 down-regulated. In total, 12,180 DEGs were identified during the grafting process, among which, 1499 genes were detected at all comparisons (Fig 1). The number of DEGs in 30d/0d was greater than 8d/0d and 15d/0d indicating the involvement of complex molecular responses during the developmental stage of vascular tissue formation.

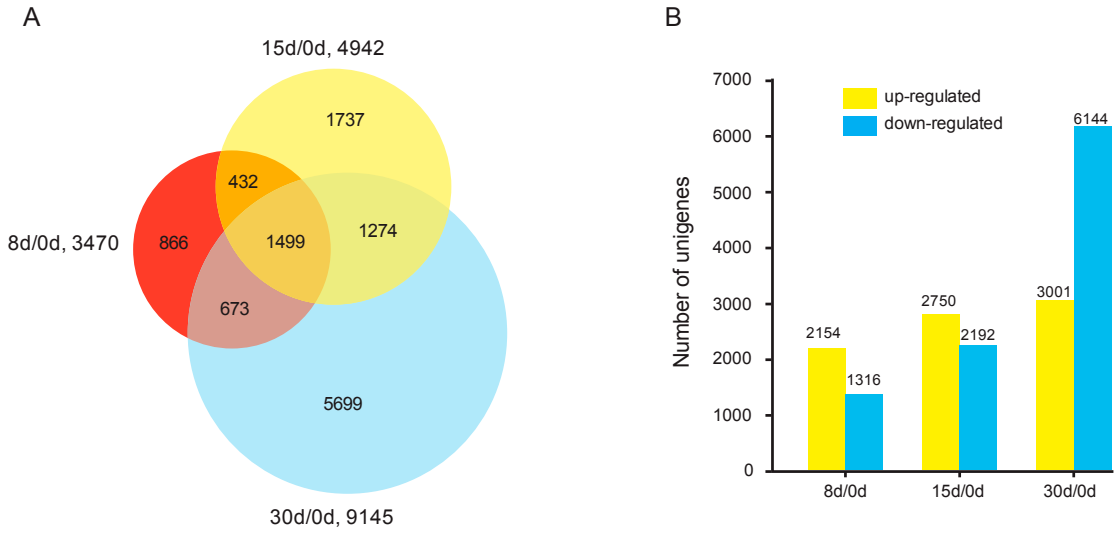

Figure 1. The DEGs in different comparisons (8d/0d, 15d/0d, and 30d/0d) during graft union development in pecan homografts.

3.3. Gene ontology and pathway enrichment analyses of DEGs

To elucidate the associated biological processes in which the DEGs were involved, the enrichment of GO terms was analyzed. For the ontology of biological process, there were 44, 28, and 38 GO enriched terms in the comparisons of 8d/0d, 15d/0d, and 30d/0d, respectively (Table S3, Fig 2). We found that 'response to hormone', 'response to oxidative stress', and 'regulation of cell cycle' were simultaneously enriched in all the comparisons, suggesting the critical roles of those biological processes for a successful grafting. Interestingly, GO terms related to 'plant-type secondary cell wall biogenesis' and 'lignin metabolic process' were specially enriched in the 30d vs 0d comparison, which were in good agreements with the developmental stage of vasculature formation at 30d.

Preprints (www.preprints.org) | NOT PEER-REVIEWED | Posted: 7 December 2017 doi:10.20944/preprints201712.0048.v1

Peer-reviewed version available at Genes 2018, 9, 71; doi:10.3390/genes9020071

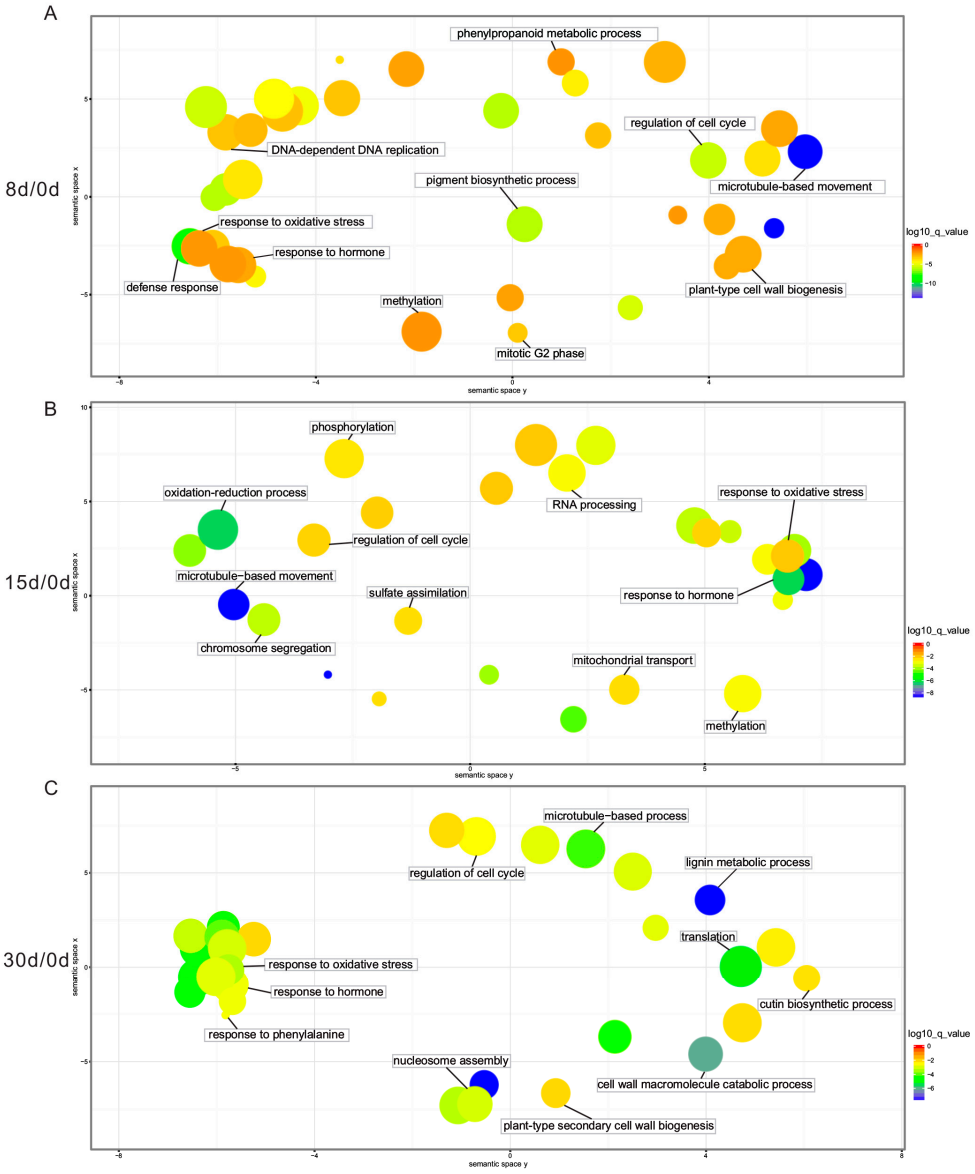

Figure 2. GO enrichment of DEGs during the graft process. (A) Significantly enriched GO terms between 8d and 0d; (B) significantly enriched GO terms between 15d and 0d; (C) significantly enriched GO terms between 30d and 0d. Bubbles represented the significant GO terms, and the bubble color gradient represented the magnitude of enrichment corresponding to q-values, while the bubble size represented the frequency of GO terms in the GOA database [13].

Additionally, KEGG enrichment analysis was performed to reveal the relevant metabolic pathways in which DEGs participated. We identified 7, 5, 2 significant enriched pathways in 8d/0d, 15d/0d and 30d/0d comparisons, respectively (Fig 3). Among those, 'phenylpropanoid biosynthesis' was the overlapping pathway that identified in three comparisons, which was consistent with the significant role of this metabolic pathway during the grafting process [10,14].

Preprints (www.preprints.org) | NOT PEER-REVIEWED | Posted: 7 December 2017 doi:10.20944/preprints201712.0048.v1

Peer-reviewed version available at Genes 2018, 9, 71; doi:10.3390/genes9020071

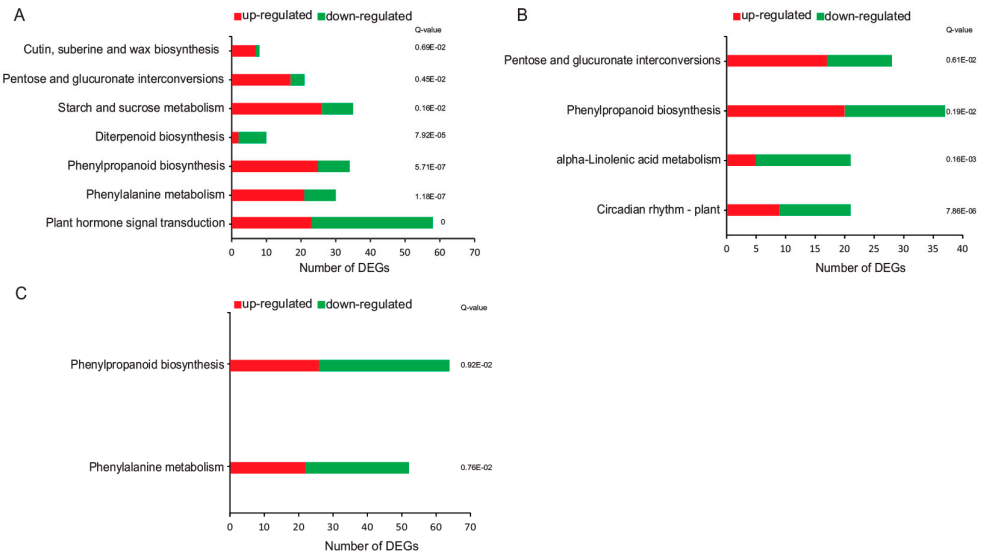

Figure 3. Significant enriched KEGG pathways during the graft process. (A) Comparison of 8d/0d; (B) comparison of 15d/0d; (C) comparison of 30d/0d.

3.4. Hormones were critical regulators for graft union development

During the grafting process, a block in auxin basipetal transport would produce due to vasculature damage, which leads to auxin accumulation at the graft junction. In our study, the content of auxin was increased distinctly at 8d, 15d and 30d after grafting (Fig 4A). Correspondingly, all the unigenes except one, c147017.graph_c0, encoding auxin influx carrier and 2 unigenes, c129281.graph_c0 and c94763.graph_c0, encoding auxin efflux carrier were significantly up-regulated over the course of graft union development (Fig 5). Similarly, genes responsible for auxin transport were induced during the grafting process of grapevine [6] and hickory [8]. The accumulated auxin is indispensable for the regulation of callus proliferation and cambial activity [15,16]. High level of auxin would release the transcriptional activity of auxin response factors (ARFs), which would induce the expression of genes that contain auxin responsive elements (AuxREs) in their promoter regions [17,18]. Previous studies reported that *ARF6* and *ARF8* mutants showed cell division defects [16], and *ARF5* mutants exhibited abnormality in vasculature development [19], indicating auxin signaling via ARFs was essential for graft union development. In the present study, six unigenes encoding ARFs were differentially expressed (Fig 5). Intriguingly, three unigenes, c37236.graph_c0, c38752.graph_c0, and c114601.graph_c0 were up-regulated significantly at 8d or 15d, indicating a specific role in callus formation; while one unigene, c142339.graph_c0, was greatly up-regulated at 30d, suggesting its pivotal role in vasculature development.

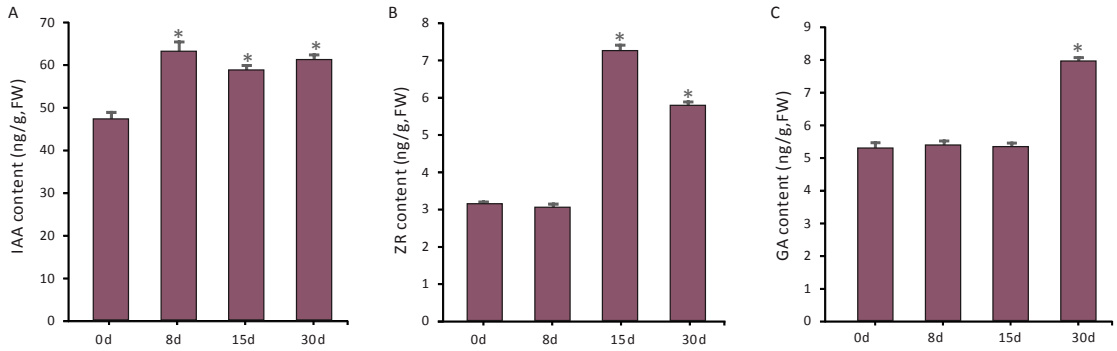

Figure 4. Determination the contents of hormone at the graft unions during the pecan grafting process. (A) Indole acetic acid (IAA), (B) zeatin riboside (ZR), and (C) gibberellic acid (GA) at different

Preprints (www.preprints.org) | NOT PEER-REVIEWED | Posted: 7 December 2017 doi:10.20944/preprints201712.0048.v1

Peer-reviewed version available at Genes 2018, 9, 71; doi:10.3390/genes9020071

time points. '*' indicated the significant differences between the specific time points and the basal level (0d).

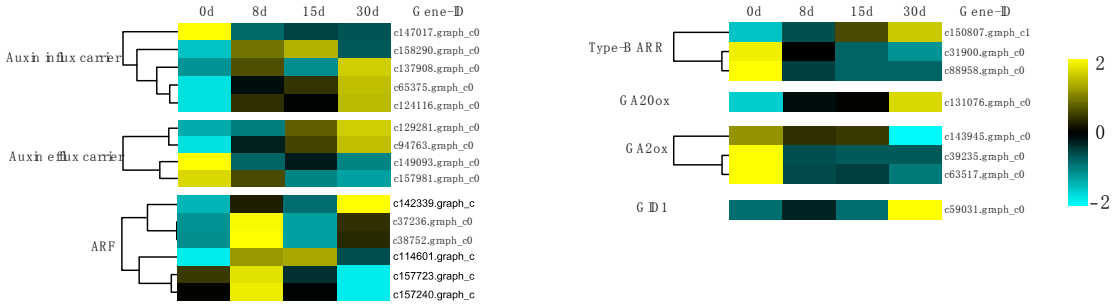

Figure 5. Expression patterns of DEGs involved in hormone signaling. Gene expression values were normalized to z-score.

Additionally, mounting evidence supports the involvement of cytokinin in cell division and vasculature differentiation [20-22]. Consistent with its role in graft union development, we found that the content of zeatin riboside (ZR), a major form of cytokinin, in graft junction was elevated significantly at 15d and 30d (Fig 4B). It is reported that although auxin is capable to stimulate cell division, cytokinin is required for its full induction [23,24]. Therefore, massive callus proliferation at 15d in this research might result from the increased cytokinin as well as auxin. Cytokinin signal transduction is mediated via two-component regulatory pathway to activate type-B ARR transcription factors [25]. Previous studies showed that triple mutants of type-B ARRs (*ARR1*, *ARR10*, *ARR12*) showed reduced callus formation [26], while overexpression of ARR1 enhanced callus formation [27].The activated type-B ARRs could be principal regulators of the cytokinin-induced callus proliferation. Three unigenes encoding type-B ARR protein were identified in our DEGs data and one of them, c150807.graph_c1, was greatly up-regulated at 15d (Fig 5), which might play an important role in callus formation. Meanwhile, cytokinin signaling was also pivotal for the regulation of cambium activity during vasculature development. Mutating cytokinin receptors, *AHK2* and *AHK3*, were reported to cause significant reduction in cambial activity [28].

More and more reports have been suggested that Gibberellin (GA) could trigger xylogenesis [29,30], which were important for the vascular bundle formation cross the grafted partners. This coincided with our biochemical analysis of GA content by ELISA, showing that GA was increased significantly at 30d, while had no significant difference at other time points (Fig 4C). Accordingly, one GA synthesis gene, *GA20ox*, were highly up-regulated after grafting and achieved its peak expression at 30d, while three GA deactivating genes, *GA2ox*, were all significantly down-regulated at 30d (Fig 5). GA signaling could promote the expression of genes involved in cell expansion as well as secondary wall biosynthesis during xylem differentiation [31,32]. For the genes involved in GA signaling, we found that one unigene encoding GID1, a gibberellin receptor, was up-regulated strikingly at 30d, which might take part in vasculature formation.

3.5. Genes responsible for callus formation

Callus formation is a basic wound response to grafting, and lack of callus production at the graft interface could lead to graft failure [33]. Genes involved in cell division are pivotal for callus formation [34]. Genome-wide transcriptomic study of callus initiation in Arabidopsis has revealed the up-regulation of various cell division related genes [35]. In this work, a considerable number of *cyclins* and *cyclin dependent kinases* (*CDKs*) associated with cell cycle were identified and all of them except one, c123028.graph_c0, were up-regulated across the grafting process (Fig 6), facilitating the activation of cellular proliferation. As aforementioned, auxin as well as cytokinin signaling play a leading role in controlling callus proliferation, because of a rate limiting factor for the G1/S transition, D-type cyclin (CYCD), is usually considered as sensor of external conditions that could be regulated by those hormone signaling [21,36,37]. Besides, many core cell cycle genes were reported to contain

Peer-reviewed version available at Genes 2018, 9, 71; doi:10.3390/genes9020071

AuxREs in their promoter regions, also demonstrating cell cycle process could be regulated by ARFs in the auxin signaling [24,36]. The induced CYCDs resulting from the accumulated auxin and cytokinin are critical for promoting cell cycle entry in our research, overexpression of which would lead to an increased callus growth rate and callus induction frequency [38].

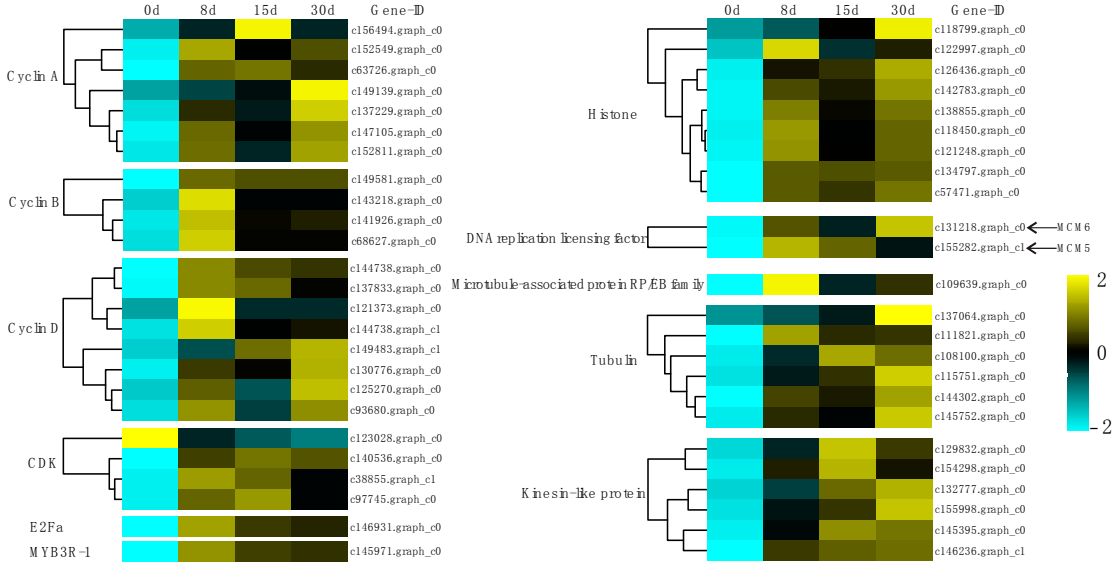

Figure 6. Expression patterns of DEGs involved in and callus formation. Gene expression values were normalized to z-score.

In addition, we found one E2Fa gene, c146931.graph_c0, and one MYB3R-1 gene, c145971.graph_c0, were up-regulated significantly during the entire period of grafting (Fig 6). E2Fa is a transcription factor that drives the expression of genes required for S-phase in cell cycle [36]. Transgenic Arabidopsis overexpressing *E2Fa* could induce cell division in tissues already devoid of proliferation [39]. MYB3R-1 is R1R2R3-type MYB transcription factor that aims at inducing genes required for M-phase in cell cycle [40]. Therefore, the up-regulated *E2Fa* along with *MYB3R1* would facilitate cell cycle progression in this study. As the entry and progress of cell cycle, numerous genes responsible for nucleosome component synthesis (*Histone*), DNA replication (*DNA replication licensing factor MCM5* and M*CM6*), microtubule cytoskeleton organization (*microtubule-associated protein RP/EB family* and *tubulin*) and cytokinesis (*Kinesin-like protein*) were generally up-regulated over the course of grafting (Fig 6), leading to callus formation.

3.6. Genes participated in vascular bundle formation

Production of new vascular tissues permits long-distance transport of nutrients between the grafting partner, and is recognized as a mark of successful grafting [33]. The sequential developmental processes underlying vascular bundle formation include promoting of vascular cambial activity, cell elongation, secondary cell wall thickening, and programmed cell death [41]. As mentioned above, auxin, cytokinin as well as GA mediated signaling are essential for the activity of vascular cambium and xylem differentiation. Following hormonal stimulation, Cells undergo significant enlargement. Enzymes such as expansions were required not only for cell growth but also for the loosening of existing cell wall architecture during cell elongation [42]. As expected, most (6 out of 7) unigenes encoding expansion in this study were up-regulated in both the callus proliferative phase and the vasculature formative phase (Fig 7). Tubulin, aside from its role in cell division, also plays a role in cell elongation by guiding nascent cellulose microfibrils deposition [43]. Expression of tubulin genes was also elevated at 30d in our study (Fig 6), potentially indicating its involvement in cell expansion.

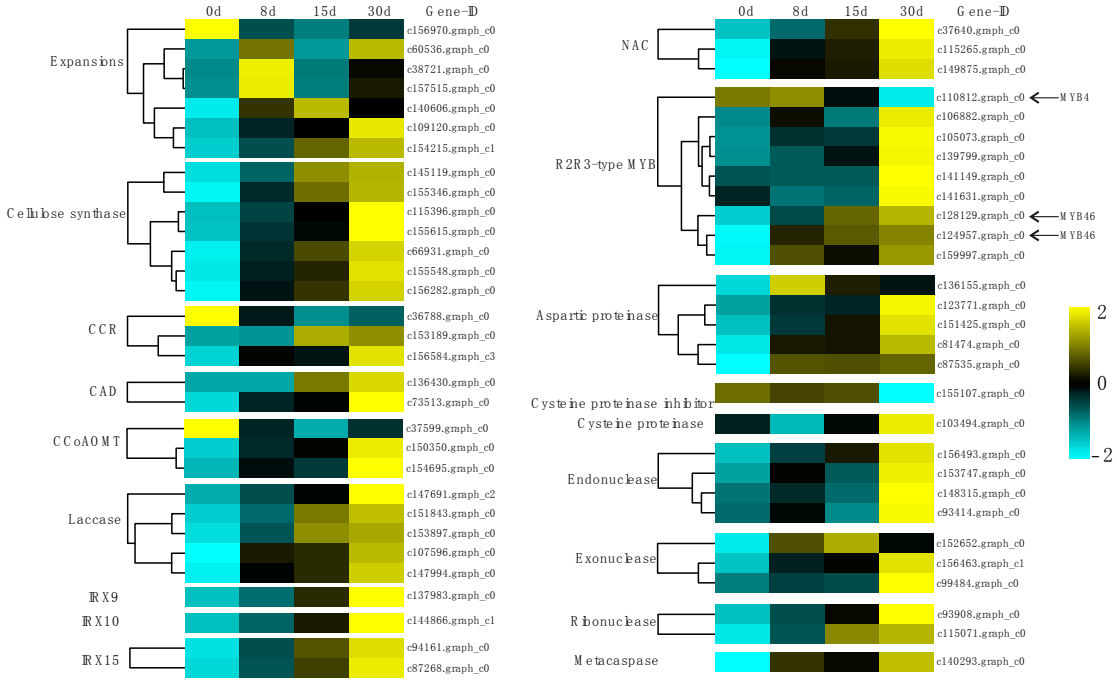

Figure 7. Expression profiles of DEGs involved in vascular bundle formation. Gene expression values were normalized to z-score.

Following completion of cell elongation, differentiating vascular cells go through deposition of cellulose, hemicellulose and lignin in the secondary cell wall. We identified various genes encoding the key biosynthetic enzymes of secondary cell wall components, and most of those genes were up-regulated with the highest expression value at 30d (Fig 7). *Cellulose synthase*, a gene implicated in cellulose synthesis, was found to be strongly expressed in the developing secondary xylem of Populus [44]. *Cinnamoyl-CoA reductase* (*CCR*), *cinnamyl-alcohol dehydrogenase* (*CAD*), and *Caffeoyl CoA 3-O-methyltransferase* (*CCoAOMT*) are the genes involved in the pheneylpropanoid pathway, all of them are critical for monolignol synthesis. The gene product of *laccase* is a polyphenol oxidase enzyme, which plays a critical role in lignin formation through inducing the oxidative polymerization of monolignols [45]. Mutations in *LACCASE4* and *17* showed reduced lignin content in *Arabidopsis* [46]. *Irregular xylem 9* (*IRX9*), *IRX10*, and *IRX15* are the genes that participate in hemicellulose synthesis.

Additionally, we identified candidate transcription factors that involved in the transcriptional regulation of secondary cell wall deposition. Some *NAC* transcription factors are master regulators in controlling the entire developmental process of secondary cell wall synthesis [47]. Overexpression of *NAC* genes in plants induced secondary wall thickening in various tissues, while repression of their function suppressed secondary wall deposition [48,49]. Three particular secondary cell wall related *NACs* were identified and all the *NACs* were strongly up-regulated at 30d (Fig 7), implying an important role during vasculature differentiation. Secondary wall related *R2R3-type MYB* transcription factors are also important regulators, which have been already identified as transcriptional regulators of phenylpropanoid biosynthesis pathway [50]. In this study, nine candidate *R2R3-type MYB* genes were found to be differentially expressed (Fig 7). Among them, two unigenes, c128129.graph_c0 and c124957.graph_c0, were annotated as *MYB46*, which act as a direct target of NAC domain regulator, exhibiting up-regulation throughout the grafting process with peak value at 30d (Fig 7). The induced *MYB46* is not only able to activate synthesis of the lignin but also the cellulose and hemicellulose [51]. One unigene, c110812.graph_c0, was annotated as *MYB4*, a gene that negatively regulated secondary cell wall formation [52], showing great down-regulation at 30d (Fig 7). Ectopic overexpression of poplar *PdYMB221*, an ortholog of *Arabidopsis* MYB4, was reported

to result in decreased thickness of cell wall [53]. Collectively, these DEGs indicated the synthesis of secondary cell wall components during vasculature differentiation.

After fulfilling secondary cell wall deposition, developing vascular cells trigger programmed cell death (PCD) to digest the cellular contents. Hydrolytic enzymes such as aspartic proteinase, cysteine proteinase and nucleases (endonuclease, exonuclease and ribonuclease) have been demonstrated to operate during xylogenesis [54-56], which were generally detected with increased expression at 30d in our research (Fig 7). Metacaspases are a class enzymes with structural similarity to animal caspases that could regulate the process of plant programmed cell death [57]. Analysis of microarray data revealed that the expression of an *Arabidopsis metacaspase 9* (*AtMC9*) homologue gene in Populus was up-regulated during xylem maturation [55]. In the present study, the great up-regulation of *metacaspase* at 30d (Fig 7) suggested its involvement in vascular bundle differentiation. Otherwise, we found one c*ysteine proteinase inhibitor* was down-regulated drastically at 30d (Fig 7), further indicating the strong activity of PCD during vascular bundle formation.

3.7. Genes involved in ROS scavenge

As a stress condition, grafting would trigger the rapid production of reactive oxygen species (ROS) in the graft interface and the accumulated ROS would function as signaling molecules to active the following antioxidant defense systems to maintain cellular redox homeostasis. For successful grafts, a high efficiency in dealing with oxidative stress is of particular importance [58-60]. In the current investigation, we found 19 DEGs that could scavenge the ROS, including genes encoding peroxidase (POD), catalase (CAT), ascorbate peroxidase (APX), cationic peroxidase and peroxiredoxin (Prx), and most of them (13 out of 15) showed increased expression during the grafting process (Fig 8), which were critical for mitigating the ROS toxicity.

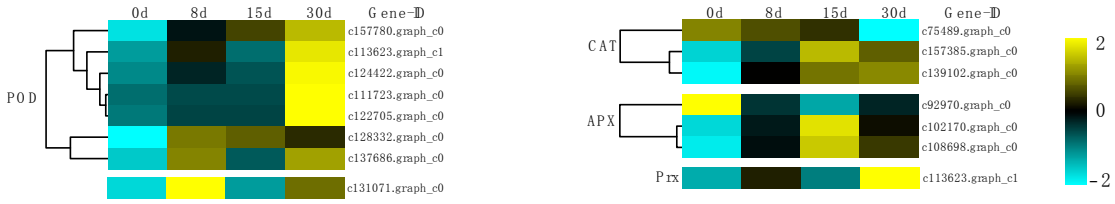

Figure 8. Expression profiles of DEGs involved in ROS scavenge (B). Gene expression values were normalized to z-score.

3.8. Validation of RNA-seq data by real-time RT-PCR

We selected twelve genes that were predicted to be associated with hormone signaling, cell division, secondary cell wall formation, programmed cell death and ROS scavenging, to validate the sequencing data. Results showed that the degree of differential expression between the two data sets did not match exactly, while the expression patterns were basically identical for those selected genes (Fig 9).

Preprints (www.preprints.org) | NOT PEER-REVIEWED | Posted: 7 December 2017 doi:10.20944/preprints201712.0048.v1

Peer-reviewed version available at Genes 2018, 9, 71; doi:10.3390/genes9020071

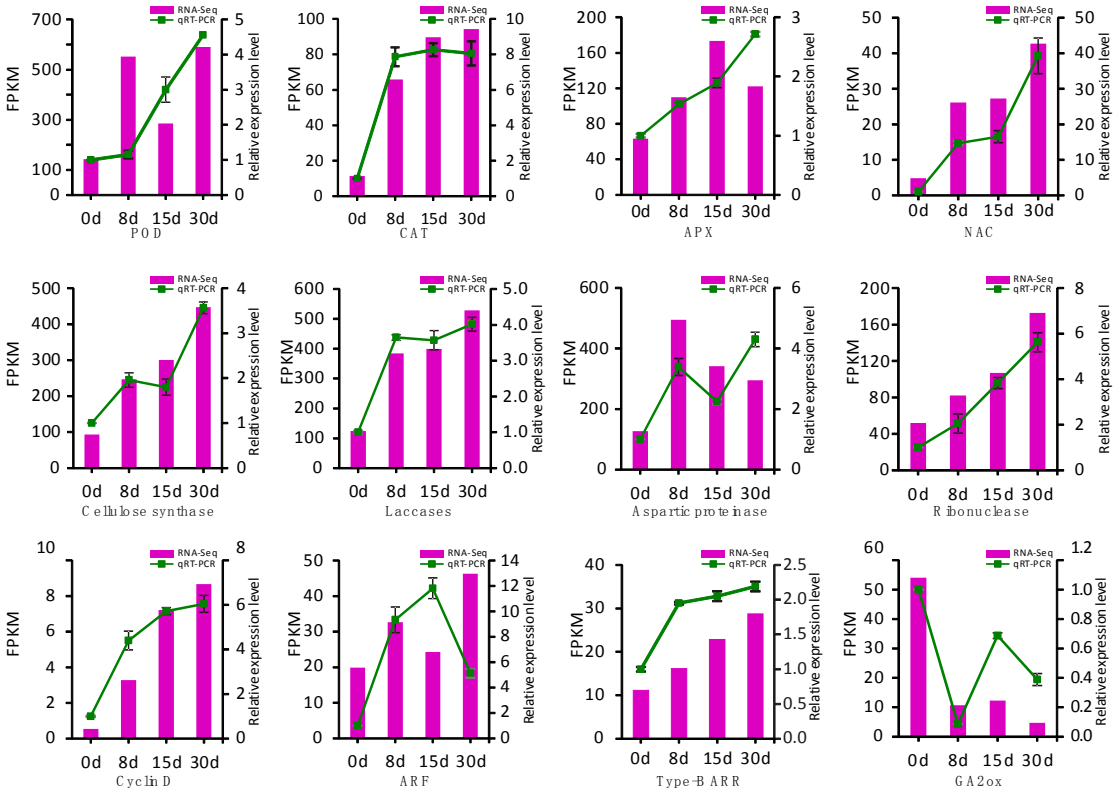

Figure 9. Validation RNA-seq data by real-time quantitative RT-PCR. The right y-axis indicated the expression level (FPKM) of RNA-seq, and the left y-axis represented the expression level of qRT-PCR.

4. Conclusion

In this work, transcriptomic analysis was applied to explore the differentially expressed genes at the graft union during the pecan homograft process. A total of 12,180 DEGs were identified at the comparisons of 8d/0d, 15d/0d and 30d/0d. Candidate genes that would participate in successful grafting were further analyzed. Based on our result, a model was proposed to elucidate the molecular mechanism of graft union development (Fig 10). In this model, auxin, cytokinin, and excessive ROS were accumulated at the graft union due to mechanical damage, and GA was produced during vasculature differentiation. As a result of that, ROS signaling might active the expression of ROS scavenge related genes to maintain cellular redox balance. Auxin and cytokinin signaling via activating ARF and type-B ARR, respectively, would regulate the expression of numerous genes related to cell division, cell elongation, secondary cell wall synthesis and programmed cell death, while GA signaling mainly regulated those genes involved in vasculature development.

Peer-reviewed version available at Genes 2018, 9, 71; doi:10.3390/genes9020071

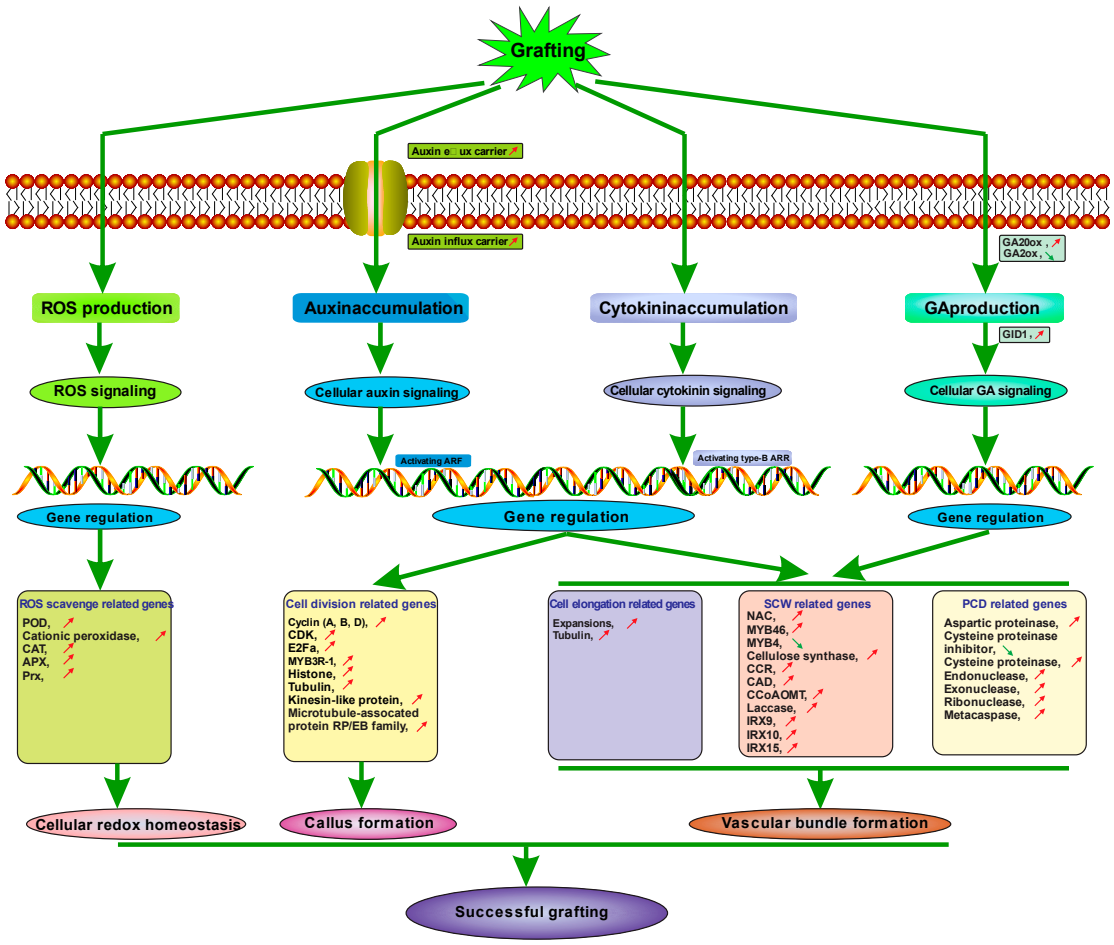

Figure 10. A putative molecular model of successful grafting in pecan. In this model, grafting induced the accumulation of ROS, auxin, cytokinin as well as the production of gibberellin at the graft interface. Then the ROS and hormones would trigger signaling pathways to modulate the expression of specific genes sets, including those responsible for ROS scavenge, cell division, cell elongation, secondary cell wall synthesis, and programmed cell death. The upper arrow indicated that most unignenes coding for the specified protein were up-regulated at the corresponding developmental stages, and the down arrow represented most unigenes were down-regulated.

Supplementary Materials: The following are available online, Figure S1: Functional categories of assembled unigenes. (A) Distribution of number of annotated unigenes in COG database; (B) Distribution of number of annotated unigenes in GO database, Figure S2: Distribution of correlation co-efficiencies between each pair of samples, Table S1: The primer sequences of selected unigenes, Table S2: Summary of sequences analysis in all samples, Table S3: Significant enriched GO terms of DEGs between different developmental stages.

Acknowledgments: The authors appreciate the financial support from the SanXin project of Jiangsu province (LYSX[2016]44), the state bureau of forestry 948 project (2015-4-16) and the Priority Academic Program Development of Jiangsu Higher Education Institutions (PAPD).

Author Contributions: F.P. conceived and designed the study. Z.M. performed the entire data analysis, carried out qRT-PCR and wrote the manuscript. G.F. and W.S. participated in hormone detection. Z.L. was involved in sample collection. All authors read and approved the final manuscript.

Conflicts of Interest: The authors declare that they have no competing interests.

References

1. Zhang, R.; Peng, F.; Li, Y. Pecan production in china. *Sci. Hortic.* **2015**, *197*, 719-727.

2. Asante, A.; Barnett, J. Graft union formation in mango (mangifera indica l.). *J. Hortic. Sci.* **1997**, *72*, 781-790.
3. YANG, Z.J.; FENG, J.L.; CHEN, H. Study on the anatomical structures in development of the nurse seed grafted union of camellia oleifera. *Plant Sci. J.* **2013**, *31*, 313-320.
4. Zheng, B.S.; Chu, H.L.; Jin, S.H.; Huang, Y.J.; Wang, Z.J.; Chen, M.; Huang, J.Q. Cdna-aflp analysis of gene expression in hickory (carya carthayensis) during graft process. *Tree physiol.* **2009**, *30*, 297-303.
5. Yin, H.; Yan, B.; Sun, J.; Jia, P.; Zhang, Z.; Yan, X.; Chai, J.; Ren, Z.; Zheng, G.; Liu, H. Graft-union development: A delicate process that involves cell–cell communication between scion and stock for local auxin accumulation. *J. Exp. Bot.* **2012**, *63*, 4219-4232.
6. Cookson, S.J.; Clemente Moreno, M.J.; Hevin, C.; Nyamba Mendome, L.Z.; Delrot, S.; Trossatmagnin, C.; Ollat, N. Graft union formation in grapevine induces transcriptional changes related to cell wall modification, wounding, hormone signalling, and secondary metabolism. *J. Exp. Bot.* **2013**, *64*, 2997-3008.
7. Cookson, S.J.; Moreno, M.J.C.; Hevin, C.; Mendome, L.Z.N.; Delrot, S.; Magnin, N.; Trossat-Magnin, C.; Ollat, N. Heterografting with nonself rootstocks induces genes involved in stress responses at the graft interface when compared with autografted controls. *J. Exp. Bot.* **2014**, *65*, 2473-2481.
8. Qiu, L.; Jiang, B.; Fang, J.; Shen, Y.; Fang, Z.; RM, S.K.; Yi, K.; Shen, C.; Yan, D.; Zheng, B. Analysis of transcriptome in hickory (carya cathayensis), and uncover the dynamics in the hormonal signaling pathway during graft process. *BMC Genomics* **2016**, *17*, 935.
9. Sima, X.; Jiang, B.; Fang, J.; He, Y.; Fang, Z.; Saravana Kumar, K.M.; Ren, W.; Qiu, L.; Chen, X.; Zheng, B. Identification by deep sequencing and profiling of conserved and novel hickory micrornas involved in the graft process. *Plant Biotechnol. Rep.* **2015**, *9*, 115-124.
10. Xu, D.; Yuan, H.; Tong, Y.; Zhao, L.; Qiu, L.; Guo, W.; Shen, C.; Liu, H.; Yan, D.; Zheng, B. Comparative proteomic analysis of the graft unions in hickory (carya cathayensis) provides insights into response mechanisms to grafting process. *Front. Plant Sci.* **2017**, *8*.
11. Mo, Z.; He, H.; Su, W.; Peng, F. Analysis of differentially accumulated proteins associated with graft union formation in pecan (carya illinoensis). *Sci. Hortic.* **2017**, *224*, 126-134.
12. Yang, Y.M.; Xu, C.N.; Wang, B.M.; Jia, J.Z. Effects of plant growth regulators on secondary wall thickening of cotton fibres. *Plant Growth Regul.* **2001**, *35*, 233-237.
13. Supek, F.; Bošnjak, M.; N, Š.; T, Š. Revigo summarizes and visualizes long lists of gene ontology terms. *Plos One* **2011**, *6*, e21800.
14. Pina, A.; Errea, P. Differential induction of phenylalanine ammonia-lyase gene expression in response to in vitro callus unions of prunus spp. *J. Plant Physiol.* **2008**, *165*, 705-714.
15. Melnyk, C.W.; Schuster, C.; Leyser, O.; Meyerowitz, E.M. A developmental framework for graft formation and vascular reconnection in arabidopsis thaliana. *Curr. Biol.* **2015**, *25*, 1306-1318.
16. Pitaksaringkarn, W.; Ishiguro, S.; Asahina, M.; Satoh, S. Arf6 and arf8 contribute to tissue reunion in incised arabidopsis inflorescence stems. *Plant Biotechnol.* **2014**, *31*, 49-53.
17. Li, S.B.; Xie, Z.Z.; Hu, C.G.; Zhang, J.Z. A review of auxin response factors (arfs) in plants. *Front. Plant Sci.* **2016**, *7*.
18. Mattsson, J.; Ckurshumova, W.; Berleth, T. Auxin signaling in arabidopsis leaf vascular development. *Plant Physiol.* **2003**, *131*, 1327-1339.
19. Hardtke, C.S.; Berleth, T. The arabidopsis gene monopteros encodes a transcription factor mediating embryo axis formation and vascular development. *EMBO J.* **1998**, *17*, 1405-1411.
20. Aloni, R.; Aloni, E.; Langhans, M.; Ullrich, C. Role of cytokinin and auxin in shaping root architecture: Regulating vascular differentiation, lateral root initiation, root apical dominance and root gravitropism.

443 *Ann. Bot.* **2006**, *97*, 883-893.
444 21. Ikeuchi, M.; Sugimoto, K.; Iwase, A. Plant callus: Mechanisms of induction and repression. *Plant Cell* **2013**,
445 *25*, 3159-3173.
446 22. Nieminen, K.; Immanen, J.; Laxell, M.; Kauppinen, L.; Tarkowski, P.; Dolezal, K.; Tähtiharju, S.; Elo, A.;
447 Decourteix, M.; Ljung, K. Cytokinin signaling regulates cambial development in poplar. *P. Natl. Acad. Sci.*
448 *USA.* **2008**, *105*, 20032-20037.
449 23. Del Pozo, J.C.; Lopez-Matas, M.; Ramirez-Parra, E.; Gutierrez, C. Hormonal control of the plant cell cycle.
450 *Physiol. Plant.* **2005**, *123*, 173-183.
451 24. Perrot-Rechenmann, C. Cellular responses to auxin: Division versus expansion. *Cold Spring Harb. Perspect.*
452 *Biol.* **2010**, *2*, a001446.
453 25. Pils, B.; Heyl, A. Unraveling the evolution of cytokinin signaling. *Plant Physiol.* **2009**, *151*, 782-791.
454 26. Mason, M.G.; Mathews, D.E.; Argyros, D.A.; Maxwell, B.B.; Kieber, J.J.; Alonso, J.M.; Ecker, J.R.; Schaller,
455 G.E. Multiple type-b response regulators mediate cytokinin signal transduction in arabidopsis. *Plant Cell*
456 **2005**, *17*, 3007-3018.
457 27. Sakai, H.; Honma, T.; Aoyama, T.; Sato, S.; Kato, T.; Tabata, S.; Oka, A. Arr1, a transcription factor for genes
458 immediately responsive to cytokinins. *Science* **2001**, *294*, 1519-1521.
459 28. Hejátko, J.; Ryu, H.; Kim, G.T.; Dobešová, R.; Choi, S.; Choi, S.M.; Souček, P.; Horák, J.; Pekárová, B.; Palme,
460 K. The histidine kinases cytokinin-independent1 and arabidopsis histidine kinase2 and 3 regulate vascular
461 tissue development in arabidopsis shoots. *Plant Cell* **2009**, *21*, 2008-2021.
462 29. Mauriat, M.; Moritz, T. Analyses of ga20ox- and gid1-over-expressing aspen suggest that gibberellins play
463 two distinct roles in wood formation. *Plant J.* **2009**, *58*, 989-1003.
464 30. Ragni, L.; Nieminen, K.; Pacheco-Villalobos, D.; Sibout, R.; Schwechheimer, C.; Hardtke, C.S. Mobile
465 gibberellin directly stimulates arabidopsis hypocotyl xylem expansion. *Plant Cell* **2011**, *23*, 1322.
466 31. Guo, H.; Wang, Y.; Liu, H.; Hu, P.; Jia, Y.; Zhang, C.; Wang, Y.; Gu, S.; Yang, C.; Wang, C. Exogenous ga3
467 application enhances xylem development and induces the expression of secondary wall biosynthesis
468 related genes in betula platyphylla. *Int. J. Mol. Sci.* **2015**, *16*, 22960-22975.
469 32. Israelsson, M.; Sundberg, B.; Moritz, T. Tissue-specific localization of gibberellins and expression of
470 gibberellin-biosynthetic and signaling genes in wood-forming tissues in aspen. *Plant J.* **2005**, *44*, 494-504.
471 33. Pina, A.; Errea, P. A review of new advances in mechanism of graft compatibility–incompatibility. *Sci.*
472 *Hortic.* **2005**, *106*, 1-11.
473 34. Chen, C.C.; Fu, S.F.; Lee, Y.I.; Lin, C.Y.; Lin, W.C.; Huang, H.J. Transcriptome analysis of age-related gain
474 of callus-forming capacity in arabidopsis hypocotyls. *Plant Cell Physiol.* **2012**, *53*, 1457-1469.
475 35. Xu, K.; Liu, J.; Fan, M.; Xin, W.; Hu, Y.; Xu, C. A genome-wide transcriptome profiling reveals the early
476 molecular events during callus initiation in arabidopsis multiple organs. *Genomics* **2012**, *100*, 116-124.
477 36. Fehér, A.; Magyar, Z. Coordination of cell division and differentiation in plants in comparison to animals.
478 *Acta Biologica Szegediensis* **2015**, *59*, 275-289.
479 37. Riou-Khamlichi, C.; Huntley, R.; Jacqmard, A.; Murray, J.A. Cytokinin activation of arabidopsis cell
480 division through a d-type cyclin. *Science* **1999**, *283*, 1541-1544.
481 38. Cockcroft, C.E.; den Boer, B.G.; Healy, J.S.; Murray, J.A. Cyclin d control of growth rate in plants. *Nature*
482 **2000**, *405*, 575.
483 39. De, V.L.; Beeckman, T.; Beemster, G.T.; De, A.E.J.; Ormenese, S.; Maes, S.; Naudts, M.; Van, D.S.E.; Jacqmard,
484 A.; Engler, G. Control of proliferation, endoreduplication and differentiation by the arabidopsis e2fa-dpa
485 transcription factor. *EMBO J.* **2002**, *21*, 1360-1368.

40. Magyar, Z.; Bögre, L.; Ito, M. Dreams make plant cells to cycle or to become quiescent. *Curr. Opin. Plant Biol.* **2016**, *34*, 100-106.
41. Ye, Z.; Zhong, R. Molecular control of wood formation in trees. *J. Exp. Bot.* **2015**, *66*, 4119-4131.
42. Ye, Z.H. Vascular tissue differentiation and pattern formation in plants. *Annu. Rev. Plant Biol.* **2002**, *53*, 183-202.
43. Mendu, N.; Silflow, C.D. Elevated levels of tubulin transcripts accompany the ga3-induced elongation of oat internode segments. *Plant Cell Physiol.* **1993**, *34*, 973-983.
44. Suzuki, S.; Li, L.; Sun, Y.H.; Chiang, V.L. The cellulose synthase gene superfamily and biochemical functions of xylem-specific cellulose synthase-like genes in populus trichocarpa. *Plant Physiol.* **2006**, *142*, 1233-1245.
45. Zhao, Q.; Nakashima, J.; Chen, F.; Yin, Y.; Fu, C.; Yun, J.; Shao, H.; Wang, X.; Wang, Z.-Y.; Dixon, R.A. Laccase is necessary and nonredundant with peroxidase for lignin polymerization during vascular development in arabidopsis. *Plant Cell* **2013**, *25*, 3976-3987.
46. Berthet, S.; Demont-Caulet, N.; Pollet, B.; Bidzinski, P.; Cézard, L.; Le Bris, P.; Borrega, N.; Hervé, J.; Blondet, E.; Balzergue, S. Disruption of laccase4 and 17 results in tissue-specific alterations to lignification of arabidopsis thaliana stems. *Plant Cell* **2011**, *23*, 1124-1137.
47. Zhong, R.; Lee, C.; Zhou, J.; McCarthy, R.L.; Ye, Z.-H. A battery of transcription factors involved in the regulation of secondary cell wall biosynthesis in arabidopsis. *Plant Cell* **2008**, *20*, 2763-2782.
48. Mitsuda, N.; Iwase, A.; Yamamoto, H.; Yoshida, M.; Seki, M.; Shinozaki, K.; Ohme-Takagi, M. Nac transcription factors, nst1 and nst3, are key regulators of the formation of secondary walls in woody tissues of arabidopsis. *Plant Cell* **2007**, *19*, 270-280.
49. Zhou, J.; Zhong, R.; Ye, Z. Arabidopsis nac domain proteins, vnd1 to vnd5, are transcriptional regulators of secondary wall biosynthesis in vessels. *PloS one* **2014**, *9*, e105726.
50. Stracke, R.; Werber, M.; Weisshaar, B. The r2r3-myb gene family in arabidopsis thaliana. *Curr. Opin. Plant Biol.* **2001**, *4*, 447-456.
51. Yang, J.H.; Wang, H. Molecular mechanisms for vascular development and secondary cell wall formation. *Front. Plant Sci.* **2016**, *7*.
52. Zhao, Q.; Dixon, R.A. Transcriptional networks for lignin biosynthesis: More complex than we thought? *Trends Plant Sci.* **2011**, *16*, 227-233.
53. Mccarthy, R.L.; Zhong, R.Q.; Fowler, S.; Lyskowski, D.; Piyasena, H.; Carleton, K.; Spicer, C.; Ye, Z.H. The poplar myb transcription factors, ptrmyb3 and ptrmyb20, are involved in the regulation of secondary wall biosynthesis. *Plant Cell Physiol.* **2010**, *51*, 1084-1090.
54. Iliev, I.; Savidge, R. Proteolytic activity in relation to seasonal cambial growth and xylogenesis in pinus banksiana. *Phytochemistry* **1999**, *50*, 953-960.
55. Courtois-Moreau, C.L.; Pesquet, E.; Sjödin, A.; Muñiz, L.; Bollhöner, B.; Kaneda, M.; Samuels, L.; Jansson, S.; Tuominen, H. A unique program for cell death in xylem fibers of populus stem. *Plant J.* **2009**, *58*, 260-274.
56. Iakimova, E.T.; Woltering, E.J. Xylogenesis in zinnia (zinnia elegans) cell cultures: Unravelling the regulatory steps in a complex developmental programmed cell death event. *Planta* **2017**, 1-25.
57. Petzold, H.E.; Zhao, M.; Beers, E.P. Expression and functions of proteases in vascular tissues. *Physiol. Plant.* **2012**, *145*, 121-129.
58. Aloni, B.; Karni, L.; Deventurero, G.; Levin, Z.; Cohen, R.; Katzir, N.; Lotan-Pompan, M.; Edelstein, M.; Aktas, H.; Turhan, E. Physiological and biochemical changes at the rootstock-scion interface in graft

combinations between cucurbita rootstocks and a melon scion. *J. HORTIC. SCI. BIOTECH.* **2008**, *83*, 777-783.

59. Irisarri, P.; Binczycki, P.; Errea, P.; Martens, H.J.; Pina, A. Oxidative stress associated with rootstock–scion interactions in pear/quince combinations during early stages of graft development. *J. Plant Physiol.* **2015**, *176*, 25-35.

60. Xu, Q.; Guo, S.R.; Li, H.; Du, N.S.; Shu, S.; Sun, J. Physiological aspects of compatibility and incompatibility in grafted cucumber seedlings. *J. Am. Soc. Hort. Sci.* **2015**, *140*, 299-307.